2014 23rd International Lightning Detection Conference
18 - 19 March • Tucson, Arizona, USA
5th International Lightning Meteorology Conference
20 - 21 March • Tucson, Arizona, USA

Forecasting Lightning Activity by Using an Explicit Charging and Discharging Scheme in WRF-ARW

Alex Fierro
Cooperative Inst. for Mesoscale Meteorological Studies
University of Oklahoma and NOAA/NSSL
Norman, OK, USA
alex.fierro@noaa.gov

Don MacGorman, Ted Mansell, and Conrad Ziegler
NOAA/National Severe Storms Laboratory
Norman, OK, USA

***Abstract*—Lightning and storm electrification schemes developed previously for simulation studies using numerical cloud models have been adapted to work with the microphysics of the operational Advanced Research Weather Research and Forecasting model (WRF-ARW). Lightning forecasts were evaluated in benchmark cases using convection-allowing (3 km horizontal grid spacing) model simulations of three contrasting convective systems: a continental squall line, a major hurricane (Rita 2005), and a winter storm. The areal coverage and magnitude of the simulated hourly flash origin density for the continental squall line were qualitatively comparable to that observed by a total lightning detection system. As was observed, no flashes were produced in the simulated winter storm case. The simulated spatial pattern of flash origin density of the hurricane and the gross charge structure in the eyewall were both in reasonable agreement with observations.**

Keywords—lightning forecast, lightning, numerical weather prediction, electrification

I. Introduction

With advances in understanding of storm electrification, it has become possible to consider forecasting lightning activity. Previous efforts have produced lightning forecasts by using relationships with other storm properties found by various studies. McCaul et al. (2009), for example, has proposed a lightning flash density prediction method whereby lightning in the convective region is assumed to be proportional to the updraft mass flux of the precipitating ice particles (graupel) in the "mixed-phase region" defined as the layer between the 0°C and -15°C isotherm (similar to Petersen et al. 1999). They further devised a second proxy that accounts for lightning occurrence in stratiform areas whereby lightning density is a function of the vertically integrated ice mass, as reported in several analyses (e.g., Zipser and Lutz 1994; Petersen et al. 1996, 1999, 2005; Cecil et al. 2005). Lynn et al. (2012) devised a dynamic lightning prediction algorithm whereby lightning rates are assumed proportional to the so-called potential electrical energy computed through diagnostic relationships between bulk cloud properties and the vertical velocity field.

Here we report on a different approach that includes explicit electrification processes in a numerical weather prediction model. This scheme uses parameterizations of both electrification and lightning production developed for storm simulation studies using numerical cloud models (e.g., Ziegler and MacGorman 1994, MacGorman et al. 2001, Mansell et al. 2002). As described in more detail by Fierro et al. (2013), these parameterizations have been adapted to work with the microphysics of the operational Advanced Research Weather Research and Forecasting model (WRF-ARW, Skamarock and Klemp 2007). The computational cost of this approach is approximately 10% over the cost of using numerical weather prediction models that do not explicitly include electrification. Further work is needed to evaluate whether the benefits of are enough to justify its use instead of using proxies for lightning production, as in previous approaches. At a minimum, our more explicit method provides a means for testing and refining approaches based on proxies.

II. Model Description

A. Electrification

The present approach parameterizes mechanisms by which hydrometeors can gain charge: noninductive charge exchange during rebounding collisions of rimed graupel with cloud ice (e.g., Takahashi and Miyawaki 2002; Saunders and Peck 1998, Mansell et al. 2005) and charge exchange during rebounding collisions of inductively polarized ice particles with polarized liquid droplets (Ziegler et al. 1991). Charge is separated macroscopically as different sized particles move apart by sedimentation and wind shear. Charge is conserved in the same way as mass is conserved as hydrometeors grow, evaporate, or are captured by other particles.

To calculate the electric field, the model first solves the Poisson Equation to obtain the electric potential from the distribution of net charge. The bottom and top of the model domain employ Dirichlet boundary conditions (zero potential at the ground, and fair-weather potential at the top), while the lateral boundaries employ the Neumann boundary condition

(zero normal derivatives). For a first guess solution and for the lateral boundary conditions, the fair weather electric field formulation of Gish (1944) is employed. The three components of the electric field then are given as the negative gradient of the potential. In the present implementation the model, the ambient electric field does not feed back onto the microphysics (e.g., through enhanced coalescence of oppositely charged cloud droplets).

B. Lightning

Our parameterization of the discharge process employs concepts adapted from a well-documented bulk lightning model (BLM, Ziegler et al. 1994). Lightning occurs when the maximum electric field magnitude produced by regions of net charge is $\geq E_{crit}$. At all gridpoints at which the magnitude is large enough, a discharge is centered around each initiation point and involves all points within a cylinder of fixed radius (R) extending vertically through the entire depth of the simulation domain. For cloud-scale simulations, R is typically on the order of a few kilometers (set here to R=6 km for all simulations). The simulated lightning trends on the 3-km grids employed for this study remained qualitatively similar in shape when R was varied between 2 and 12 km. If cylinders overlap, they are merged. This method gives only a rough measure of lightning activity. A more sophisticated method, such as that employed by MacGorman et al. (2001) or Mansell et al. (2002), would be needed to improve estimates of flash rates or to estimate the polarity of flashes.

To determine the charge involved in discharges during a time step, the discharge model computes the sum of the space charge within the discharge volume for all grid cells with net positive charge (S+) at which the magnitude of charge exceeds some nominal threshold (e.g., 0.1 nC m^{-3}) and, similarly, the magnitude of the sum for all cells with net negative space charge magnitude (S-) at which the magnitude exceeds the threshold. The total magnitude of charge Q_d to be superposed for each polarity is set to 30% (Ziegler and MacGorman 1994) of the maximum of S+ and S-, unless that product exceeds the summed magnitude of opposite polarity. In that exceptional case, Q_d is simply set to the lesser of S+ and S-. Then the positive charge to be superposed on each grid cell with net negative charge is given by $q_{ijk} * Q_d / S+$, and, similarly, the magnitude of negative charge superposed on each grid cell with net positive charge is given by $q_{ijk} * Q_d / S-$, where q_{ijk} is the magnitude of net space charge above the threshold at grid cell i,j,k.

The lightning charge is distributed throughout all discharge volumes during a time step by adding space charge with polarity opposite to that of the net space at each grid cell within any lightning cylinder. The magnitude of opposite-polarity space charge added at a grid cell is given by the above expressions and is distributed across all hydrometeor species in the grid cell. The magnitude placed on a specific hydrometeor species is proportional to the fraction of surface area of that species relative to the total surface area of all species in that grid cell. As explained by Ziegler and MacGorman (1994), this distribution mimics the capture of free-ion space charge by each hydrometeor species, but is done instantaneously, in the time step in which the flash occurs, rather than by explicit ion processes as done, for example, by Helsdon et al. (1992) and Mansell et al. (2005).

The discharge procedure is repeated iteratively in a time step until the maximum E_{mag} no longer exceeds E_{crit} anywhere in the domain. In other words, the discharge first determines the locations of E_{mag} exceeding E_{crit}, then redistributes the charge, and as a last step updates the electric field solution across the domain. If E_{mag} from the updated electric field solution exceeds E_{crit} anywhere in the domain the discharge process is repeated. Typically, no more than 3 iterations are required.

To establish a meaningful comparison with the output of McCaul et al.'s (2009) scheme and, therefore, to provide a lightning metric more accessible to forecasters who might wish to use the BLM output, the following operation was devised to compute an estimate of flash origin density FOD rate (over a time period T=t2-t1) per grid cell:

$$FOD(i,j,T) = \frac{G}{C}\int_{t1}^{t2} B(i,j,t)dt$$

where G is the grid cell area (in km^2 per grid-cell), C the cylinder cross sectional area (in km^2) and the integral on the right hand side (units of per time interval T) representing the sum of all flash origins in cell i,j,k for all the time steps within the time interval T. The units of FOD are in flashes per grid-cell per time.

III. Model Lightning Forecasts

To provide a reasonable evaluation of our forecast model, the simulated lightning fields were assessed for three convective systems differing drastically in their internal dynamics and thermodynamic environments: a continental squall line, a tropical cyclone and a continental winter storm.

A. Description of the Three Cases

The chief motivation behind the choice of each case study differs. For the severe continental squall line (15 April 2012) and the continental winter storm (1 January 2012) cases, the main criterion for selection was the production of a reasonable forecast of the convection with a cold start beginning at 00Z to mimic the situation under which experimental forecasts are conducted with the National Severe Storms Laboratory (NSSL) 4–km WRF-ARW testbed over the contiguous United States (CONUS). The tropical cyclone (Hurricane Rita, in September 2005) was well documented and offered an extended period with interacting thunderstorms producing lightning.

On 15 April 2012, during the late afternoon and evening hours, the collision of a retreating dryline with an eastward-moving cold front in the Texas (TX) panhandle resulted in the rapid development of a large squall-line mesoscale convective system (MCS) over northwest TX, western Oklahoma (OK), and central Kansas (KS) (Fig. 1). The merging mesoscale boundaries were reasonably well resolved in the National Centers for Environmental Prediction (NCEP) North American Model (NAM) analysis and forecast fields that were used to initialize and provide time-dependent lateral boundary conditions for experimental forecasts conducted with the NSSL

4–km WRF-ARW testbed over CONUS. Thus, the NSSL-WRF was able to forecast the timing and location of convective initiation (CI) and subsequent upscale development of this squall line with reasonable accuracy.

The formation of the squall line MCS in the model was found to lag observations by up to about 1 h (i.e., 0400 in the observations versus 0500 in the model). A likely cause for the delay in upscale development of convection to form the MCS is a delay in the timing of convective initiation owing to the use of relatively coarse initial reanalysis fields (40 km), which tend to under-resolve the sharp gradients along mesoscale boundaries such as drylines or cold fronts (e.g., as seen in Fierro et al. 2012), and the time required for mesoscale boundary layer solenoids in the initial model state to generate convergence and shear required to help force convective initiation. Simulated radar reflectivity fields of the squall line, however, show overall good agreement with the 3D NMQ observations, particularly at and after 0600 (Fig. 1). The WRF model also captures the gradual weakening of the system after 0800 as evidenced by the weakening of the simulated reflectivities. As in the observations, the simulation also reproduces the overall lack of linear organization of the convection in Kansas.

On 1 January 2012, strong northerly flow wrapping around the northern and northwestern side of a strong low pressure system over the northern Great Plains resulted in sufficient cold air advection and lift to generate a snow storm (Fig. 2). Because synoptic scale ingredients were the primary driver for this winter storm event, the NSSL 4–km WRF-ARW testbed was also able to capture the evolution of this system reasonably well. Because no lightning was detected in this winter storm during the simulation period, this case was selected to document performance in simulating a null case.

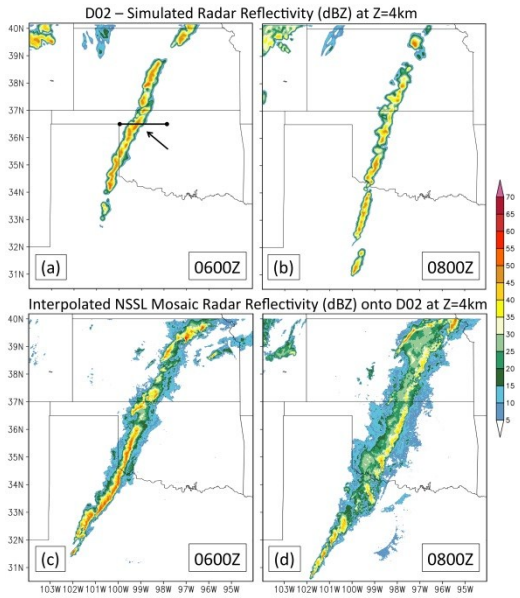

Figure 1. The top row shows horizontal crosssection of the simulated radar reflectivity at z=4 km AGL (in dBZ) at (a) 0600 and (b) 0800 UTC on April 15 2012. The bottom row is as in (a) and (b) but for 1-km resolution, three-dimensional observations from the NSSL NMQ product interpolated onto the local 3-km (D02) domain. Legends for colors and shadings are shown on the right of the figure. (from Fierro et al. 2013)

The evolution of the areal coverage and placement of the winter storm is captured reasonably well by the model between 0200Z and 1200Z (Fig. 2). There are, however, noteworthy differences to underline: first, the simulated reflectivity fields are about 5-10 dB larger than observed; second, the model develops cellular convection in northern Missouri at 0600 which was absent in the observations (Fig 2 a, c) and, third, the tail end of the simulated snow band at 0800 extends further south than observed (Fig. 2b, d). Last the snow band in the simulation is more prominent northeast of Lake Superior at 0800 (Fig. 2b, d).

Hurricane Rita was a major hurricane which made landfall on the Texas coast and in South Florida resulting in an estimate of 12 billion dollars in damage. During its journey in the Gulf of Mexico between 20 and 24 September 2005, Rita rapidly intensified from a Category 2 to a Category 5 storm, reaching maximum sustained winds near 155 kts (Knabb et al. 2005). During this rapid intensification cycle, which was centered near 1200Z on 21 September 2005, the storm experienced several lightning bursts in its eyewall, some of which were documented by several studies (Shao et al. 2005; Squires and Businger 2008 (SB08); Fierro et al. 2011 (F11)). Observations and simulations are discussed in Fierro et al. (2013), but will not be discussed here, because of limited time and space.

For this presentation, we focus only on lightning forecasts in the squall line and winter storm cases. For both the 15 April and 1 January case, the simulated FOD are compared to available total lightning observations from the Earth Networks® Total Lightning Network (ENTLN), which consists of over 150 sensors deployed over CONUS alone (http://weather.weatherbug.com/weatherbug-professional/products/total-lightning-network) able to detect both IC and CG flashes. For more details about the model set up and the

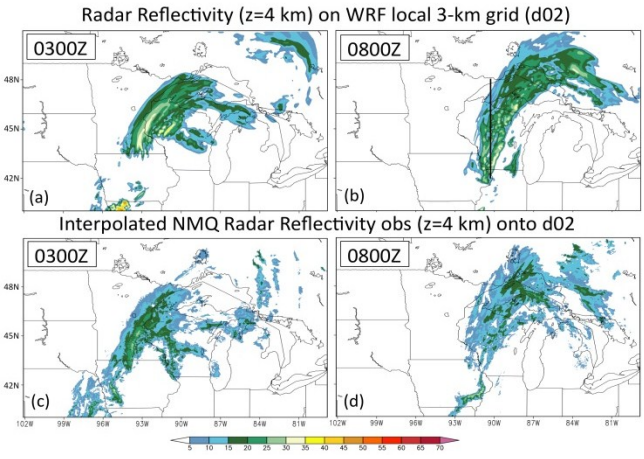

Figure 2. As in Fig. 1, but for the 1 January 2012 winter storm case at 0300 and 0800 UTC (from Fierro et al. 2013).

results of the simulations in all three cases, see Fierro et al. (2013).

B. Lightning in Squall Line on 15 April 2012

The simulation gives a reasonable reproduction of the observed storms, and the simulated 1-h accumulated FOD spatial pattern shows overall reasonable agreement with the total lightning observations from ENTLN (Fig. 3). In particular, the evolution of the simulated FOD rates exhibits a gradual decrease over OK and central KS, consistent with a weakening squall line (Fig. 1). Similar to the radar reflectivity fields, the simulated FOD also show a slight eastward displacement relative to the observations especially at 0800 (Fig. 1 and 3) as well as an overall lack of lightning activity in the southern TX panhandle compared to the observations at both times (Fig. 3). The largest differences between the BLM lightning fields and the ENTLN observations are seen at 0800 with two distinct FOD maxima in northeast KS and west central TX (102ºW-101ºW, 31ºN-32ºN), both of which are absent in the simulation (Fig. 3b, d) as evidenced by the simulated reflectivity fields (Fig. 1b, d). Overall, the simulated FOD values are in remarkably good agreement with the ENTLN densities.

Figure 4 shows the FOD from the three diagnostic schemes of McCaul et al. (2009, hereafter referred to as MC) at the same times as in Figure 3. The derived FOD values for each of the MC schemes, namely the maximum FOD per 5-min per grid cell, were multiplied by a factor 12 to provide an estimate of the upper limit of the maximum FOD h^{-1} per grid cell. The first MC scheme ("F1") is proportional to the vertical graupel mass flux at -15ºC and the second MC scheme ("F2") is proportional to the total ice mass in the column. Scheme F1 is suited for forecasting lightning near and within the updraft cores, while scheme F2 is designed to account for flashes occurring within stratiform regions. The third MC scheme ("F3") is a linear combination of F1 and F2 (i.e., 0.95 * F1 + 0.05 * F2), to account for both regions.

The overall spatial patterns of the lightning from the BLM and the MC schemes are in accord, particularly with scheme F3 (compare Figs. 3a, b and 4c, d). The difference in locations of areas of maximum lightning activity and areal coverage of the simulated FOD show overall negligible differences between the BLM and all three MC schemes (Fig. 3a vs. Fig. 4a, b, c). Quantitatively, provided that (i) the plotted MC FOD values represent an upper limit for maximum hourly rates; (ii) the constants in the MC diagnostic relationships were not specifically calibrated for 2-moment microphysics schemes; and (iii) that their lightning threats were calibrated using the Lightning Mapping Array (LMA, MacGorman et al. 2008) data and not ENTLN, their simulated values are overall in relatively good agreement with the BLM's and the ENTLN observations (e.g., Fig. 3 vs. Fig. 4). Keeping the above in mind and that the IC detection efficiency of ENTLN over OK is about 75% (see

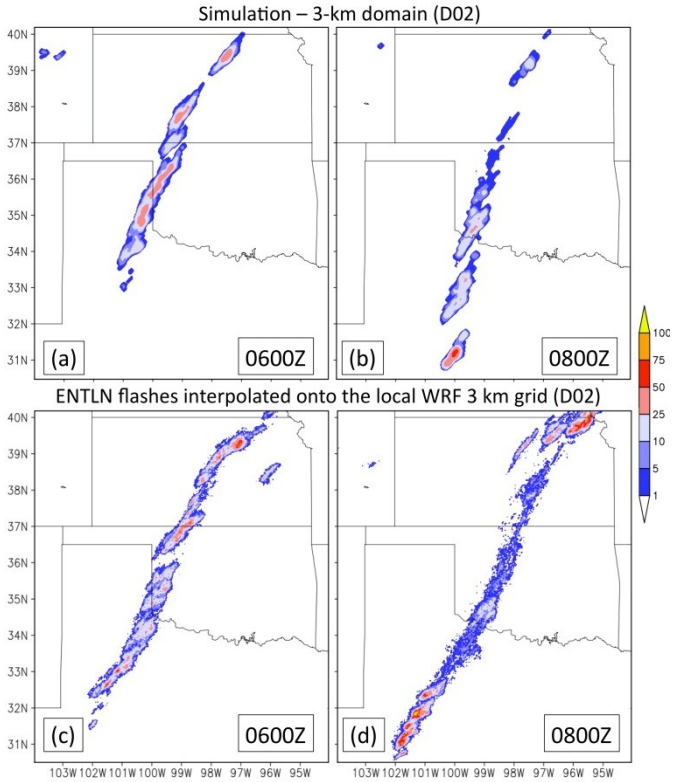

Figure 3. As in Fig. 1 but for the simulated flash origin density (FOD, per grid cell h^{-1}) with the BLM shown in (a) and (b) and the ENTLN total lightning data interpolated onto the local 3-km domain (D02) shown in (c) and (d). The FOD were summed for an hour prior to the times shown in the figures. Legends for colors and shadings are shown on the right of the figure. (from Fierro et al. 2013)

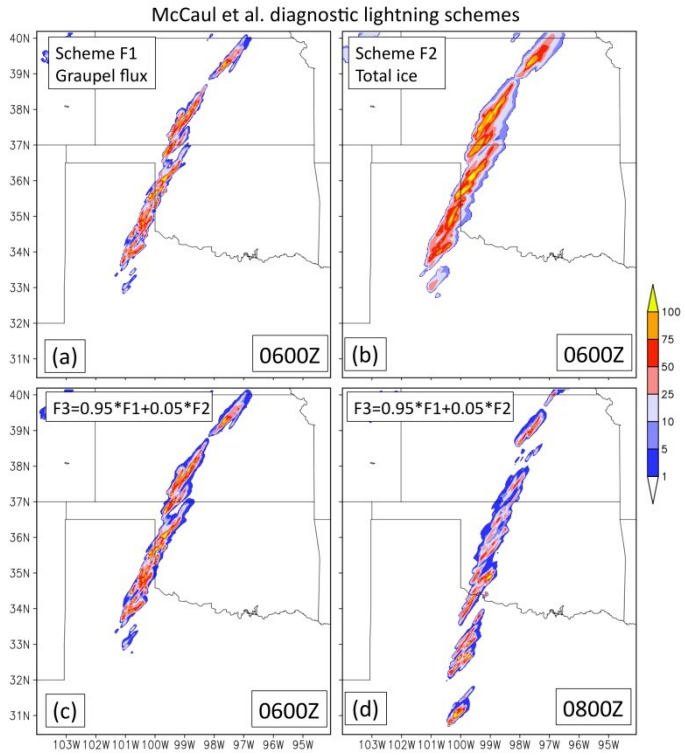

Figure 4. As in Fig. 3, but for the FOD from the McCaul et al. (2009) schemes converted to an upper limit of maximum FOD per grid-cell per hour. The top row shows those FOD at 0600 using (a) F1 and (b) F2. The bottom row shows the same fields for F3 at (c) 0600 and (d) 0800. Legends for colors and shadings are the same as in Figure 3. (from Fierro et al. 2013)

Fig. 6 in Fierro et al. 2013) some quantitative differences ought to be noted, however. For instance, at 0600 in Central OK, the BLM produces (hourly) FOD rates ranging between 25-50 in agreement with ENTLN observations (Figs. 4a, c) while the rates of MC Scheme F3 often exceed 75 (with local maxima above 100, Fig. 4c). This quantitative difference is further exacerbated during the weakening stage of the squall line: At 0800, observations show maximum FOD rates rarely exceeding 10 while MC scheme F3 generates rates often exceeding 25 in contrast to the BLM, whose FOD rates essentially remain between 10-25 (Figs. 3b, d and 4d) in closer agreement with the observations.

C. Lightning in the Winter Storm on 1 January 2012

Again the model had a reasonable reproduction of the observed reflectivity fields (Fig. 2), and the resulting BLM showed no lightning, in agreement with the ENTLN observations, (Fig. 5a, b) during the time period considered herein (i.e., 0200 to 1200). Although small, the MC schemes, on the other hand, show non-zero FOD values on the order of 1 per grid cell per hour (Fig 5c, d shown for scheme F3). This is because, at the time of this experiment, the MC scheme designed for stratiform regions, namely F2 (and hence, F3), assumed the presence of lightning whenever ice and mixed-phase particles were simulated. In contrast, the BLM requires the simultaneous presence of mixed-phase particle and supercooled (LWC) water, both of which are small in the simulated winter band convection. Consistent with the reflectivity structure, the simulation had small amount of mixed phase particles, and rain and echo tops exceeded 6 km only in a convective cell on the warmer southern tip of the band. This cell was characterized by vertical velocities on the order of 1-2 m s^{-1}, graupel mixing ratios on the order of 0.01 g kg^{-1} and isolated pockets of liquid water content reaching 0.2 g m^{-3}.

Despite the BLM's lack of simulated lightning, the snow clouds exhibit some degree of electrification, with weak E_{mag} rarely reaching 50 V m^{-1}. Space charge (electric field) values were about three (four) orders of magnitudes smaller than those simulated in the continental MCS and Hurricane Rita (not shown).

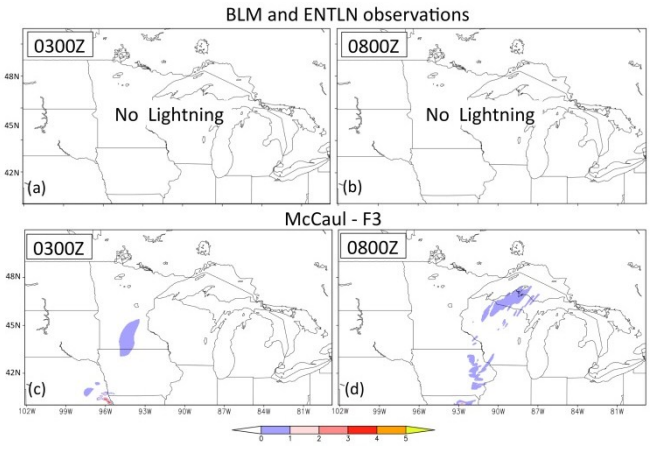

Figure 1. (a) and (b) as in Fig. 3 and (c) and (d) as in Fig. 4c, d for the 1 January 2012 winter storm case at 0300 and 0800 UTC (from Fierro et al. 2013).

IV. Discussion

The BLM demonstrated here can simulate lightning activity explicitly in a bulk sense for a wide variety of storms, and so can be used to produce lightning forecasts at a computational cost of approximately 10% over the cost of forecasts without electrification and lightning. The method of McCaul et al. (2009), which forecasts lightning through diagnostic relationships with the upward graupel mass flux and columnar ice mass output by models, produces reasonable forecasts in many situations and is computationally cheaper. Their version tested here erred in producing lightning in winter storms, but a newer version has subsequently been tuned to avoid producing lightning in weak stratiform precipitation, such as that produced in winter. The advantage of the BLM is that its forecasts are based on explicit parameterizations of electrification and lightning physics, and so do not need the same kind of tuning. However, the forecasts of both models can be no better than the forecasts of the microphysics on which they are based, and so require more sophisticated microphysical packages than those incorporated in the operational version of WRF used by the National Weather Service. However, microphysics packages are improving, and the version in WRF-ARW was adequate for the range of situations tested here and in Fierro et al. (2013).

Acknowledgments

This research was supported in part by the NOAA/Office of Oceanic and Atmospheric Research under NOAA-University of Oklahoma Cooperative Agreement #NA11OAR4320072, U.S. Department of Commerce. This work was also supported by the GOES-R program at NESDIS through NOAA award #NA08OAR4320904. Computer resources were provided by the Oklahoma Supercomputing Center for Education and Research (OSCER) hosted at the University of Oklahoma. The authors thank Scott Dembek for providing the 40-km NAM data and Ami Arthur for providing the NSSL three-dimensional NMQ radar mosaic data.

References

Cecil, D. J., S. J. Goodman, D. J. Boccippio, E. J. Zipser, and S. W. Nesbitt (2005), Three years of TRMM precipitation features. Part I: Radar, radiometric, and lightning characteristics. *Mon. Wea. Rev.*, 133, 543–566.

Fierro, A. O, X-M. Shao, J. M. Reisner, J. D. Harlin and T. Hamlin (2011), Evolution of eyewall convective events as indicated by intra-cloud and cloud-to-ground lightning activity during the rapid intensification of Hurricanes Rita and Katrina. *Mon. Wea. Rev.,* **139**, 1492-1504.

Fierro, A. O., E. Mansell, C. Ziegler, D. MacGorman (2012), Application of a lightning data assimilation technique in the WRF-ARW model at cloud-resolving scales for the tornado outbreak of 24 May 2011. *Mon. Wea. Rev.*, 140, 2609-2627.

Fierro, A. O., E. R. Mansell, D. R. MacGorman, and C. L. Ziegler (2013), The implementation of an explicit charging and lightning scheme within the WRF-ARW model: Benchmark simulations of a continental squall line, a tropical cyclone, and a winter storm. *Mon. Wea. Rev.*, 141, 2390–2415, doi: 10.1175/MWR-D-12-00278.1.

Gish, O. H. (1944), Evaluation and interpretation of the columnar resistance of the atmosphere, *Terr. Magn. Atmos. Electr.*, 49, 159–168.

Helsdon, J. H., Jr., G. Wu, and R. D. Farley (1992), An intracloud lightning parameterization scheme for a storm electrification model, *J. Geophys. Res.*, 97, 5865–5884.

Knabb, R. D., J. R. Rhome, and D. P. Brown: Tropical cyclone report (2005), Hurricane Rita. Technical report, National Hurricane Center, National

Oceanographic and Atmospheric Administration, Available at http://www.nhc.noaa.gov/2005atlan.shtml.

Lynn B. H., Yair Y., Price C., Kelman G. and A. J. Clark (2012), Predicting cloud-to-ground and intracloud lightning in weather forecast models. *Wea. and Forecasting*, 27, 1470-1488, doi: 10.1175/WAF-D-11-00144.1

MacGorman, D. R., J. M. Straka and C. L. Ziegler, (2001), A lightning parameterization for numerical cloud models. *J. Appl. Meteor.*, 40, 459–478.

MacGorman, D. R., D. Rust, T. Schuur, M. Biggerstaff, J. Straka, C. Ziegler, E. Mansell, E. Bruning, K. Kuhlman, N. Lund, N. Biermann, C. Payne, L. Carey, P. Krehbiel, W. Rison, K. Eack, W. Beasley, (2008), TELEX: The Thunderstorm Electrification and Lightning Experiment. *Bull. Amer. Meteor. Soc.*, **89**, 997-1013, doi: 10.1175/2007BAMS2352.1.

Mansell, E. R., D. R. MacGorman, C. L. Ziegler and J. M. Straka (2002), Simulated three-dimensional branched lightning in a numerical thunderstorm model. *J. Geophys. Res.*, 107, 4075, doi: 10.1029/2000JD000244.

Mansell, E. R., D. R. MacGorman, C. L. Ziegler and J. M. Straka (2005), Charge structure and lightning sensitivity in a simulated multicell thunderstorm. *J. Geophys. Res.*, 110, D12101, doi: 10.1029/2004JD005287.

McCaul, E. W., S. J. Goodman, K. M. LaCasse and D. J. Cecil (2009), Forecasting lightning threat using cloud-resolving model simulations. *Wea. Forecasting*, 24, 709–729.

Petersen, Walter A., Steven A. Rutledge, Richard E. Orville (1996), Cloud-to-ground lightning observations from TOGA COARE: Selected results and lightning location algorithms. *Mon. Wea. Rev.*, 124, 602–620.

Petersen, W. A., R. C. Cifelli , S. A. Rutledge , B. S. Ferrier , and B. F. Smull (1999), Shipborne dual-doppler operations and observations during TOGA COARE., *Bull. Amer. Meteor. Soc.*, 80, 81-97

Petersen, W. A., H. J. Christian, and S. A. Rutledge (2005), TRMM observations of the global relationship between ice water content and lightning, *Geophys. Res. Lett.*, 32, L14819, doi:10.1029/2005GL023236.

Saunders, C. P. R., and S. L. Peck (1998), Laboratory studies of the influence of the rime accretion rate on charge transfer during crystal/graupel collisions. J. Geophys. Res., 103, 13949–13956.

Shao, X. M., J. Harlin, M. Stock, M. Stanley, A. Regan, K. Wiens, T. Hamlin, M. Pongratz, D. Suszcynsky, and T. Light (2005), Katrina and Rita were lit up with lightning, *EOS Trans., AGU*, **86**, 398, doi: 10.1029/2005EO420004.

Skamarock, W. C., and J. B. Klemp (2007), A time-split nonhydrostatic atmospheric model for research and weather and forecasting. *J. Comput. Phys.*, 227, 3465–3485.

Squires, K., and S. Businger (2008), The morphology of eyewall lightning outbreaks in two category 5 hurricanes. *Mon. Wea. Rev*., **136**, 1706–1726.

Takahashi, T., and K. Miyawaki (2002), Reexamination of riming electrification in a wind tunnel, *J. Atmos. Sci.*, 59, 1018–1025

Ziegler, C. L., D. R. MacGorman, J. E. Dye, and P. S. Ray (1991), A model evaluation of non-inductive graupel-ice charging in the early electrification of a mountain thunderstorm. *J. Geophys. Res.*, 96, 12 833–12 855.

Ziegler, C. L. and D. R. MacGorman (1994), Observed lightning morphology relative to modeled space charge and electric field distributions in a tornadic storm. *J. Atmos. Sci.*, 51, 833–851.

Zipser E. J., and K. Lutz (1994), The vertical profile of radar reflectivity of convective cells: A strong indicator of storm and lightning probability? *Mon. Wea. Rev.*, 122, 1751–1759.